A Computationally Inexpensive Radio Propagation Model for Vehicular Communication on Flyovers and Inside Underpasses

Muhammad Ahsan Qureshi[1*], Ehsan Mostajeran[1], Rafidah Md Noor[1], Azra Shamim[2], Chih-Heng Ke[3]
[1] FSKTM, University of Malaya,
Kuala Lumpur, 50603, Malaysia
[2]COMSATS Institute of Information Technology,
Islamabad, Pakistan
[3]National Quemoy University
Kinmen, 892 Taiwan, R.O.C.
[e-mail: ahsanqureshi1@gmail.com, fidah@um.edu.my]
*Corresponding author: Muhammad Ahsan Qureshi

Received December 9, 2015; revised March 6, 2016; revised April 16, 2016; accepted July 22, 2016; published September 30, 2016

Abstract

Vehicular Ad Hoc Networks (VANETs) utilize radio propagation models (RPMs) to predict path loss in vehicular environment. Modern urban vehicular environment contains road infrastructure units that include road tunnels, straight roads, curved roads flyovers and underpasses. Different RPMs were proposed in the past to predict path loss, but modern road infrastructure units especially flyovers and underpasses are neglected previously. Most of the existing RPMs are computationally complex and ignore some of the critical features such as impact of infrastructure units on the signal propagation and the effect of both static and moving radio obstacles on signal attenuation. Therefore, the existing RPMs are incapable of predicting path loss in flyovers and underpass accurately. This paper proposes an RPM to predict path loss for vehicular communication on flyovers and inside underpasses that considers both the static and moving radio obstacles while requiring only marginal overhead. The proposed RPM is validated based upon the field measurements in 5 GHz frequency band. A close agreement is found between the measured and predicted values of path loss.

Keywords: Radio Propagation Model, VANETs, Static Radio Obstacles, Moving Radio Obstacles, Flyover, Underpass

1. Introduction

VANETs is a challenging field of wireless technology that utilizes vehicle to infrastructure (V2I) and vehicle to vehicle (V2V) communications to provide a wide variety of useful applications ranging from safety related applications to infotainment services [1]. IEEE 802.11p standards are widely adopted in VANETs that operate in 5.9 GHz frequency band [2]. VANETs utilize 75 MHz of 5.9 GHz spectrum to facilitate V2X (both V2V and V2I) communications for dedicated short range communication (DSRC) [3].

The modern transport infrastructure has evolved and is now comprised of road infrastructural units such as complex interchanges, flyovers, underpasses and road tunnels to support new traffic conditions. Radio signal propagation is differently affected by each of the road infrastructure unit. For instance, road infrastructure unit such as flyover serves as a static radio obstacle that impedes radio signals [4] and the radio propagation behavior is different in tunnels as compared to free space propagation [5].

The wavelength of the radio signals in 5.9 GHz frequency band is approximately 5 cm; therefore the penetrating power of these signals are low as compared to other technologies such as GSM that usually operates in 1800 MHz frequency band. Therefore, the radio obstacles that obstruct radio signals have relatively high impact in VANETs as compared to other technologies. The radio obstacles that impede radio signals in VANETs include static and moving obstacles. Static obstacle includes buildings, dense vegetation, and advertising boards [6]. However, the structure of the modern road infrastructure units may also be regarded as a potential static radio obstacle. Moving obstacles include large buses, trailers and delivery trucks that impede radio signals in VANETs [1].

The RPMs in VANETs formulize the propagation of radio signals to accurately predict behavior of radio waves [7]. A realistic RPM which is computationally inexpensive yet provides accurate prediction of path loss while covering all physical aspects of propagation and considers the modern road infrastructure units is required [8]. The existing RPMs in VANETs are developed to be used in the older road infrastructure units such as straight roads and junctions. No RPM in the literature exists that predicts path loss specifically for the communication taking place on the flyovers and inside the underpasses which are significant part of today's urban road transport environment. However, a number of RPMs [9-11] exist for the prediction of path loss in tunnels but either the field measurements are not taken in the frequency band suitable for VANETs or they lack in one or more of the critical aspect such as modelling of moving obstacles.

The impact of moving radio obstacles on propagation behavior is also amplified with the ever-increasing presence of large moving vehicles on the modern road infrastructure units. Therefore, there is a need to study the radio propagation behavior in the modern road infrastructure units especially flyovers and underpasses. The study of the impact of moving obstacles on radio propagation on flyovers and inside underpass with the field measurements close to the frequency band for VANETs facilitates more reliable communication infrastructure by providing a computationally inexpensive RPM. Furthermore, the radio reception performance is sensitive to antenna placement in the 5 GHz band [12]. Hence, the selection of antenna is important [13].

This paper proposes an RPM for V2V communication to predict accurate path loss on flyovers and inside underpasses by considering both the static and moving radio obstacles and yet having minimal overhead. The rest of the paper is organized as follows. Section 2

discusses existing RPMs for V2V communication. Section 3 presents the proposed radio propagation for flyovers and underpasses along with the mathematical formulation to calculate the impact of moving vehicles on path loss. The field measurement campaign along with the measurement results in terms of received signal strength (RSS) are discussed in Section 4. The validation of proposed RPM is explained in section 5. The comparison of the proposed and existing RPMs is presented in section 6 and Section 7 concludes the paper.

2. Existing Radio Propagation models in VANETs

Although, the RPMs employed in VANETs can be utilized in mobile ad-hoc networks; however, VANETs have their own requirements such as topological characteristics, network density and mobility style. Generally, the RPMs can be categorized in two main groups from implementation point of view, namely, deterministic RPMs and probabilistic RPMs [8]. A classification of RPMs is shown in **Fig. 1.**

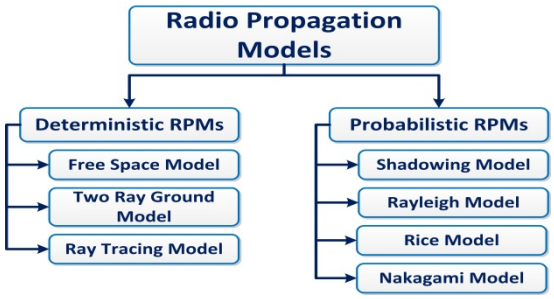

Fig. 1. Classification of RPMs

2.1 Deterministic RPMs

The path loss is calculated based upon real properties of the environment such as speed of the communicating vehicles and inter-vehiclur distance in deterministic RPMs. Deterministic RPMs fall into two groups; simple and complex according to computationally complexity. Free space and two ray ground models are the examples of deterministic RPMs [14, 15] which are widely adopted in VANETs. However, these models ignore critical aspects of the environment proving unrealistic estimation of path loss. Some of the existing RPMs are difficult to implement and computationally expensive as they focus on critical aspects of the environment such as ray tracing models [16, 17] that utilizes permittivity, conductivity, and thickness of radio obstacles etc. Consequently, complex RPMs are infrequently applied.

2.2 Probabilistic RPMs

On the other hand, a probabilistic RPM provides the path loss estimation by utilizing a simple deterministic model as input parameter and applies statistical methods to estimate the path loss. Log normal shadowing, Rayleigh and Rician fading are examples of probabilistic RPMs [18, 19]. For instance, the shadowing model introduces a random variable along with the path loss component arguing that RSS at a certain distance from the sender can only be represented by a random variable because of fading effects from multipath propagation.

2.3 Road Infrastructure Consideration in RPMs

The existing RPMs employed in VANETs mainly focus on highway or urban scenarios. However in urban scenarios, most of the existing RPMs only consider a simple junction with Manhattan style grid architecture [20-22]. For instance, CORNER **[6]** is a popular RPM that considers Manhattan style grid and implements a propagation attenuation formula presented in [23]. Therefore, no attention is given towards the study of radio propagation properties in modern road infrastructure units especially flyovers and underpasses. However, studies are conducted in the past to observe signal attenuation in tunnels. A tunnel can be considered as a waveguide due to its geometry and the conductivity [24]. According to existing research, the transverse dimensional tunnels which are much larger than the radio signal's wavelength experience waveguide properties [25, 26]. The tunnel geometry, electromagnetic properties of the tunnel's material, antenna characteristics and radio obstacles also affect the radio propagation in tunnels [24].

From the existing work on RPMs, it is identified that some of the existing RPMs are computationally complex; others are not validated for the widely utilized frequency band for VANETs; most of the existing RPMs do not consider additional attenuation from the large moving objects; and none of the existing RPMs are focused on flyovers and underpasses. Therefore, a computationally inexpensive RPM with minimal number of parameters for vehicular communication for flyovers and underpass is required that is validated in the allowed frequency band for VANETs and accounts for the additional signal attenuation that may result from moving radio obstacles on the flyover and inside an underpass.

3. Proposed RPMs for Flyover and Underpasses

This section describes the simple and computationally inexpensive RPMs suitable for predicting path loss on flyovers and inside underpasses. These RPMs are validated based upon extensive field measurement campaign. Our goal is to propose such an RPM that utilizes a minimal set of parameters to estimate path loss in an acceptable range. The following subsections provide detail on proposed RPMs for flyover and underpass respectively.

3.1 Proposed RPM for Flyover

The architecture of a flyover makes it a potential static radio obstacle for the communicating vehicles. Two sorts of communication occur among the vehicles while driving on the flyover; (a) line-of-sight (LOS) communication and (b) non line-of-sight (NLOS) [27] communication. The communicating vehicles are in LOS with each other when at least one the vehicle (transmitter/receiver) is either travelling on the highest point along the flyover or it is currently at a relatively higher position on the flyover as compared to the other communicating vehicle. However, the LOS between two communicating vehicles may be disturbed by large moving radio obstacles that may appear between the communicating vehicles. The vehicles travelling on the opposite ends of the flyover loose LOS among them due to the height of the structure. The structure of the flyover is the cause of NLOS condition among the communicating vehicles in this scenario. This phenomenon is explained in **Fig.2**. Here, the green straight line represents LOS communication and red line shows the NLOS scenario. The pillars of the flyover and the concrete base at the ends of the flyover are potential static radio obstacles for the vehicular communication.

In case of LOS communication among the vehicles on the flyover, the free-space model can be utilized for the prediction of path loss in LOS scenario if the additional attenuation due

to large moving radio obstacle on the flyover is also considered. Therefore, the total path loss in LOS scenario on the flyover is dependent upon two factors; (a) free space path loss ($\boldsymbol{PL_{freespace}}$) and (b) the additional attenuation due to the presence of the large moving radio obstacle ($\boldsymbol{PL_{AM}}$).

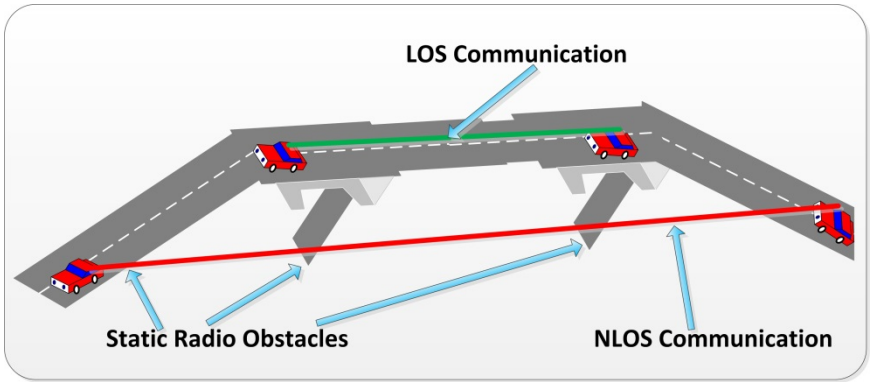

Fig. 2. Types of Communication in Flyovers

The maximum path loss due to the presence of large moving radio obstacles is estimated using single knife-edge effect. The single knife-edge model can be applied in the situations where the wavelength of the radio signal is significantly smaller than the size of the radio obstacle [1]. An approximation of the additional path loss in dB caused by the moving radio obstacles in vehicular communication can be represented using equation 1.

$$PL_{AM}[dB] = 6.9 + 20log_{10}\left[\sqrt{(v-0.1)^2+1} + v - 0.1\right] \quad (1)$$

Where

$$v = \sqrt{2}\,\frac{H}{r_f} \quad (2)$$

In equation 2, $\boldsymbol{H}$ denotes the difference between the height of the radio obstacle and the height of the straight line connecting the communicating vehicles. The presence of the radio obstacle within 60% of the first Fresnel's zone ellipsoid is the cause of the additional attenuation. Therefore, equation 2 includes a parameter $\boldsymbol{r_f}$ [1]; which is the radius of the first Fresnel's zone ellipsoid and is obtained by the following equation.

$$r_f = \sqrt{\frac{\lambda d_{obs}(d - d_{obs})}{d}} \quad (3)$$

In equation 3, $\boldsymbol{d}$ is the distance between communicating vehicles (Tx and Tr) and $\boldsymbol{d_{obs}}$ is the distance between the obstacle and Tx.

However, the additional attenuation due to moving radio obstacles is also dependent upon the frequency $\boldsymbol{F}$ of the large radio obstacles in the overall traffic. The formula for the calculation of total LOS path loss for the vehicular communication while the nodes are travelling on the flyover is given by the equation 4.

$$PL_{LOS}\,[dB] = PL_{TS}\,[dB] = PL_{freespace}\,[dB] + F(PL_{AM}[dB]) \quad (4)$$

Where $\boldsymbol{PL_{AM}\ [dB]}$ is described in equation 1 and $\boldsymbol{F}$ represents the probability of the large moving obstacles to disturb the LOS among the communicating vehicles. $\boldsymbol{PL_{freespace}}$ is the free space path loss in dB as expressed in equation 5 where $\boldsymbol{f}$ denotes the frequency of the radio signal.

$$PL_{freespace}[dB] = 20\log_{10}(d) + 20\log_{10}(f) + 32.44 - G_t - G_r \quad (5)$$

The general model for path loss prediction is to be extended to contemplate the impact of flyover structure on the vehicular communication. Therefore, the NLOS scenario for the vehicular communication that arises due to the architecture of the flyover is modelled by capturing additional attenuation caused by the structure of the flyover. This additional attenuation is modelled by calculating ***n***; the number of times the LOS is obstructed by the static radio obstacles (pillars and flyover edges). A collaboration factor $\boldsymbol{\beta}$ is introduced to represent the additional signal attenuation in dB caused by individual static radio obstacles present in the structure of the flyover (pillars and flyover edges). The additional attenuation due to the structure of the flyover $\boldsymbol{PL_{AF}[dB]}$ is given in equation 6.

$$PL_{AF}\,[dB] = n\beta \quad (6)$$

The additional attenuation $\boldsymbol{PL_{AF}}$ is combined with the free-space model to elucidate the total path loss $\boldsymbol{PL_{NLOS}}$ in NLOS scenario for the flyover. The $\boldsymbol{PL_{NLOS}}$ is calculated as shown in equation 7.

$$PL_{NLOS}[dB] = PL_{freespace}[dB] + \; PL_{AF}[dB] \quad (7)$$

The total path loss in flyover $\boldsymbol{PL_{TF}}$ as explained in equation 8 either represented by equation 4 for LOS scenario or it is represented by equation 7 for NLOS scenario. The LOS scenario represents a situation where the structure of the flyover has no effect on the LOS of the communicating vehicles. However, the LOS among the communicating vehicles may be disturbed occasionally by the presence of moving radio obstacles in the LOS scenario.

$$PL_{TF} = \begin{cases} PL_{LOS} & If\ LOS\ communication \\ PL_{NLOS} & If\ NLOS\ communication \end{cases} \quad (8)$$

3.2 Proposed RPM for Underpass

The underpass is a sort of a small tunnel incorporated in an effort to make modern urban road transport environment signal free. The typical length of the underpass varies from 20 meters to 60 meters depending upon the width of the road that runs on top of the underpass orthogonally. Due to relatively short length of underpass as compared to road tunnel, it is likely that only one of the transmitting or receiving vehicles is inside the underpass at the time of the communication while the other vehicle may be travelling outside the underpass. Moreover, a scenario might exist where both the communicating vehicles are present outside on two different ends of the underpass. Hence three possible scenarios are to be considered when proposing the propagation formula to predict path loss for the underpasses. The three possible scenarios are; (a) both the communicating vehicles are inside the underpass, (b) only one of the communicating vehicles is inside the underpass and (c) both the communicating vehicles are outside on two different ends of the underpass.

The path loss in underpass is logarithmically proportional to the distance between the communicating nodes, therefore,

$$PL_M[dB] = k\ log_{10}(d) \quad (9)$$

In equation 9, $\boldsymbol{PL_M}$ denotes the major component of path loss, $\boldsymbol{d}$ is the distance between communicating vehicles. The constant of proportionality is $\boldsymbol{k}$, determined by using the dimensions of the underpass and wavelength of the radio signal. The formula for the calculation of $\boldsymbol{k}$ is shown in Equation 10.

$$k = r + \frac{w}{h\lambda} \tag{10}$$

In equation 10, $\boldsymbol{r}$ represents the absolute value of the difference of height and width of the road tunnel ($|\boldsymbol{w}$-$\boldsymbol{h}|$); where $\boldsymbol{w}$ and $\boldsymbol{h}$ are width and height of the road tunnel respectively. Equation 10 can be used to calculate k if $\boldsymbol{w} > \boldsymbol{h}$. However, if $\boldsymbol{h} > \boldsymbol{w}$, then the value of $\boldsymbol{k}$ is calculated as ($\boldsymbol{r} + \boldsymbol{h}/\boldsymbol{w\lambda}$) [28].

The impact of moving radio obstacles on the radio propagation is already formulated in section 3.1. The approximation for the total path loss in "scenario a" of the underpass $\boldsymbol{PL_{TT}}$ is the combination of $\boldsymbol{PL_M}$ and $\boldsymbol{PL_{AM}}$ as given in equation 11.

$$PL_{TT}\,[dB] = PL_M[dB] + F(PL_{AM}[dB]) \tag{11}$$

In equation 11, $\boldsymbol{PL_M}$ denotes the major component of path loss. A novel approach of calculating the effective distance $\boldsymbol{d_{eu}}$ between communicating vehicles to predict path loss for the vehicular communication in and outside the underpass is adopted in this research. The advantage in the strength of the received signal gained as a result of waveguide effect due to the structure of the underpass can be modeled by calculating the effective distance $\boldsymbol{d_{eu}}$ between the communicating vehicles. The effective distance $\boldsymbol{d_{eu}}$ is the calculated distance between the sender and receiver such that a portion of the distance travelled by the radio signal inside the underpass is subtracted from actual straight line distance $\boldsymbol{d}$ between the communicating vehicles. Therefore, the effective distance $\boldsymbol{d_{eu}}$ is always less than the actual straight line distance d between the sender and the receiver ($\boldsymbol{d_{eu}} < \boldsymbol{d}$). The portion of the distance which is subtracted from d to yield $\boldsymbol{d_{eu}}$ is proportional to the area of cross-section of the underpass because the waveguide effect is phenomenal only in those tunnels/underpasses whose transverse dimensions are several times greater than the wavelength of the radio signal [25]. The effective distance $\boldsymbol{d_{eu}}$ is expressed in equation 12.

$$d_{eu} = d - l_{eu}\left(1 - \frac{\sqrt{w^2 + h^2}}{A_{cu}}\right) \tag{12}$$

In equation 12, $\boldsymbol{l_{eu}}$ is the effective length of the underpass starting from the point where one of the communicating vehicles is present and ends at the outer edge of the underpass towards the other communicating vehicle in case when one of the communicating vehicles is inside the underpass (scenario b). However, $\boldsymbol{l_{eu}}$ equals to the exact length of the underpass in case wherein both the communicating vehicles are outside the underpass on different ends (scenario c). In equation 9, w and h represents the width and height of the underpass respectively and $\boldsymbol{A_{cu}}$ represents the area of cross-section of the underpass.

The total path loss $\boldsymbol{PL_{TU}}$ in scenarios b and c for the underpass can be represented by equation 13.

$$PL_{TU}[dB] = PL_{fs(d_{eu})}[dB] + F(PL_{AM}[dB]) \tag{13}$$

In equation 13, $\boldsymbol{PL_{fs(deu)}}$ represents the free space path loss by considering $\boldsymbol{d_{eu}}$ as the distance between the sender and the receiver.

The vehicular communication is not substantially affected by the static radio obstacles in the underpass simply because of the inexistence of static obstacle that can cause severe change

in the signal attenuation. Therefore, in equation 13, PL_{AM} *[dB]* is the only additional signal attenuation components caused by the moving radio obstacles.

3.3 Computational Complexity of the Proposed RPM

The propagation formula for the flyover consisted of two components; (1) free space path loss and (2) additional attenuation caused by the moving radio obstacles (LOS scenario) / additional attenuation due to structure of the flyover (NLOS scenario). The calculation of additional attenuation due to the moving radio obstacles in simulation is the most expensive step because it involves at least an O(m log m + k) line intersection algorithm **[29]** for computing k intersections among m lines. However, the maximum signal attenuation is calculated only once. The probability F of the moving obstacles to disturb LOS among communicating vehicles is multiplied with the maximum signal attenuation caused by moving obstacles in order to reasonably estimate the additional path loss. Therefore, the calculation of additional attenuation due to moving radio obstacles becomes an algorithm with a constant running time. Furthermore, the additional attenuation due to flyover's structure (nβ) is again calculated in constant time. In the underpass propagation formula, the total path loss is composed of two factors namely, (1) major path loss and (2) additional attenuation due to moving radio obstacles. The major path loss is calculated using the geometric properties of the underpass. Hence, calculation of the major path loss in underpass is an O(n) algorithm for n number of communications. Hence, the proposed RPMs are computationally inexpensive.

4. Measurement Campaign

4.1 Equipment and Setup

An extensive data gathering campaign was carried out at sixth road flyover (Rawalpindi, Punjab, Pakistan, latitude: 33.6424722 longitude: 73.0714255) using 802.11 n WiFi devices configured at 5 GHz. The length of the sixth road flyover is a 462 meters with 3 lanes on each side of the road. It is part of a very busy urban road in a densely populated city situated in north of Pakistan. For the underpass, we selected the committee chowk underpass (Rawalpindi, Punjab, Pakistan, latitude: 33.6108749 longitude: 73.0651639). The length of the underpass is approximately 27 meters with two lanes on each side of the road. The width of the under pass on one side of the road is 9 meters and height is approximately 6 meters separated by a concrete wall in between the two roads. The communicating nodes consist of Intel Dual Band Wireless-N 7265 wireless adapter connected to a D-Link ANT70-0800 omnidirectional antenna that provided a gain of 10dBi at 5Ghz. The antenna was connected with the wireless device using a cable of length 3 m (~ 3 dB loss). We utilize Garmin GPS 18x USB receiver for locating the position of nodes. The vehicles used in the experiment were Honda city 2007 (height: 1495 mm) and Suzuki Mehran (height: 1410 mm). The antenna and the GPS receiver were mounted on the roof of the vehicles.

4.2 Measurement Scenarios (Flyover)

In the simplest of arrangements, one vehicle (Tx) was parked on the left lane at the start of the flyover and the RSS was measured using the other vehicle (Tr) driven at very low speed. In another scenario, the RSS is measured while Tx was stationary and Tr was driven at 40 km/hr and the test is repeated at 60 km/hr. Both vehicles were driven at same speed (30 km/hr) while maintaining a distance of 150 meters, 200 meters and 250 meters respectively from each other in three of the subsequent arrangements. In one of the arrangements, both vehicles were

driven at variable speeds is such a manner that one vehicle approaches the other vehicle with greater speed and then leaves it behind for the rest of measurement. **Table 1** shows multiple scenarios used for the measurement of RSS on the flyover.

Table 1. Measurement Scenarios (Flyover)

Scenario	Tx Speed	Tr Speed	Updation	Inter-vehicular Distance	Orientation
FSC1	Stationary	5 km/hr	1 meters	Variable	Tr going away from Tx
FSC2	Stationary	40 km/hr	5 meter	Variable	Tr going away from Tx
FSC3	Stationary	60 km/hr	5 meter	Variable	Tr going away from Tx
FSC4	30 km/hr	30 km/hr	5 meters	150 meters	A constant distance is maintained
FSC5	30 km/hr	30 km/hr	5 meters	200 meters	A constant distance is maintained
FSC6	30 km/hr	30 km/hr	5 meters	250 meters	A constant distance is maintained
FSC7	30 km/hr	60 km/hr	~8 meters	variable	Tr approaching Tx and then going away

4.3 Measurement Scenarios (Underpass)

In the first arrangement, Tx was parked just before the start of the underpass in the left lane. Tr is driven at very low speed (5 km/hr) inside the underpass to carefully monitor the fluctuation in the RSS values. In order to check the impact of vehicle's speed variation on the RSS values, the same test is repeated USC2 while Tx was stationary and Tr was driven at 30 km/hr. In USC3, both the vehicles were driven at same speed (20 km/hr) while maintaining a distance of 15 meters. The arrangement of USC3 is repeated in USC4 by driving both the vehicles with the same speed while maintaining a distance of 25 meters between them. In both the scenarios (USC3 and USC4), the vehicles maintained the LOS between them while driving inside the underpass because the selected underpass consisted of a street road. In the last of the measurement scenarios, vehicles were driven at different speeds in such a manner that Tx is ahead of Tr at the beginning of the test on the straight road. Tx enters the underpass and continue its journey with relatively low speed as compared to Tr. Therefore, Tr approaches Tx with greater speed and then overtakes it inside the underpass. Tr continue to move further away from Tx for the rest of the test as both the vehicles leave the underpass behind. **Table 2** shows multiple scenarios used for the measurement of RSS inside underpass.

Table 2. Measurement Scenarios (Underpass)

Scenario	Tx Speed	Tr Speed	Updation	Inter-vehicular Distance	Orientation
USC1	Stationary	5 km/hr	1 meter	Variable	Tr going away from Tx
USC2	Stationary	20 km/hr	1 meters	Variable	Tr going away from Tx
USC3	10 km/hr	10 km/hr	~2 meters	15 meters	A constant distance is maintained
USC4	20 km/hr	20 km/hr	~2 meters	25 meters	A constant distance is maintained
USC5	15 km/hr	30 km/hr	~4 meters	variable	Tr approaching Tx and then going away

4.4 Experimental Results

The communication performance at flyover and inside underpass was analyzed using the measured RSS and its dependency on the distance between the communicating nodes in multiple arrangements. We utilized path loss as another performance indicator to summarize the results as shown in **Table 3.**

Table 3. Performance indicators

Performance Indicator	Unit	Typical Value Range
RSS	dBm	-110 to -10
Path Loss	dB	5 to 140

Fig. 3 shows the RSS as measured in FSC1 where Tx was kept stationary at the start of the flyover and Tr was driven at a very low speed to acquire RSS value after each meter along the flyover. A sudden decrease in RSS (15dBm to 20dBm) was observed when the vehicles were no longer in LOS with each other. The decrease in RSS in NLOS scenario is due to the additional attenuation caused by the concrete structure of the flyover as Tx was parked at the start of the flyover and Tr was present at a certain height where there was no LOS between the two communicating vehicles. This decrease in RSS was observed when the distance between the communicating vehicles exceeded 150 meters and is shown by the red circle in **Fig. 3.**

Due to the extreme load of traffic on the flyover, the measurement in FSC1 was taken using the left lane of the flyover. The pillars of the flyover have minimal effect on LOS on communicating vehicles in the left lane due to the structure of the flyover. The radio signals quickly deteriorate when NLOS scenario arises. However, the decrease in the RSS was gradual when Tr is present at relatively higher altitude. When the distance between the communicating vehicles exceeds (approximately 310 meters), the connection between Tx and Rx was lost because Rx start to descend and the LOS is now disturbed due the concrete structure causing further attenuation that result in the perishing of the connection.

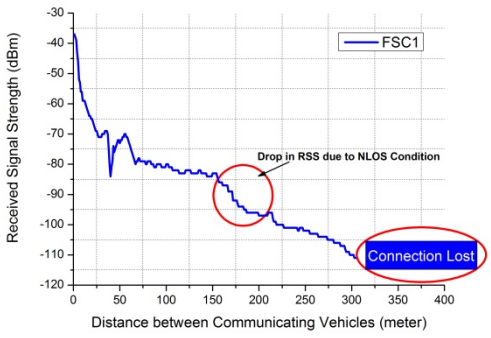

Fig. 3. RSS in FSC1

In the next two scenarios (FSC2 and FSC3), the tests were conducted to observe the impact of variable speeds of Tr on signal attenuation. However, the RSS values in FSC2 and FSC3 are no different than the values observed in FSC1 as shown in **Fig. 4**. Therefore, the variable speeds of Tr have no significant effect on the signal attenuation. The results of FSC2 and FSC3 also endorsed the results obtained in FSC1 that maintaining the LOS between the communicating vehicles on the flyover ensures reliable connection because the strength of radio signals quickly deteriorates in case of NLOS scenario. The RSS measurements in the

next three scenarios (FSC4, FSC5 and FSC6) were taken to observe the impact of flyover's structure on the signal attenuation by maintaining a constant distance between the communicating vehicles and driving both vehicles at with the same speed. In this manner, a deep apprehension of decline in the signal strength due to the flyover's structure is cognizance.

In FSC4, the RSS values were recorded when the Tx and Tr were in LOS at the beginning of test because a distance of 150 meters was maintained between them. Tx was at lower point on the flyover as compared to Tr in the beginning of the test. As the vehicles were driven along the flyover, they started to lose the LOS. Therefore, a steady decline in the RSS values was observed. However, the radio signals became stronger when Tx and Tr again came in LOS with each other while driving at the highest points over the flyover. The rise in the signal strength can be observed when both the vehicles have travelled about 150 meters as shown in **Fig. 5** and **Fig. 6.** The decline in RSS was again observed when the vehicles lose LOS but this time Tx was at a higher point as compared to Tr.

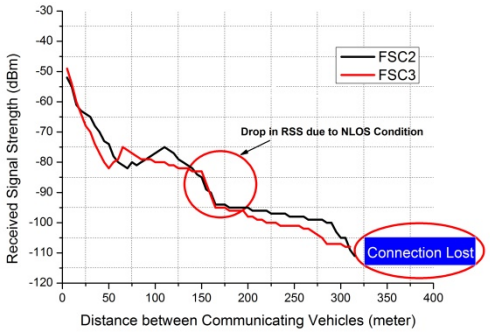

Fig. 4. RSS in FSC2 and FSC3

The arrangement of vehicles in FSC4 was again repeated in FSC5, however, the distance maintained between Tx and Tr was 200 meters in FCS5. At the start of the test, the vehicles (Tx and Tr) were not in LOS with each other. Therefore, an RSS of approximately -100dBm was observed at the start of the test. As the vehicles move on, they gradually begin to come within the LOS with each other, hence, resulting in a steady increase at the start of the test. The increase in the RSS in FSC5 was persistent up to the point where both the vehicles were at the highest points on the flyover. However, a decrease in RSS was observed when Tr started to descend and the vehicles were no longer in LOS with other as shown in **Fig. 6.** In FSC6, Tx and Tr were not in LOS with each other at the start of the test. After the vehicles travelled approximately 80 meters along the flyover, the connection was lost. This is due to the fact that both the vehicles were on lower points on opposite ends of the flyover. Therefore, the LOS between Tx and Tr was disturbed more than once due to the structure of the flyover that results in the connection lost. This phenomenon is shown in **Fig. 5.**

The communicating vehicles were again connected after travelling approximately 150 meters along the flyover because the LOS was disturbed only one due to the underneath structure of the flyover. A gradual increase in RSS was observed as the communicating vehicles begin to come in LOS with each other. At the end of the test, Tx was at the highest point on the flyover and Tr was at a lower point on a straight road after the flyover. Therefore, the communicating vehicles were in LOS with each other at the end of the test. Hence, an increased RSS value (~ -88 dBm) was observed when the two vehicles have covered about 250 meter distance.

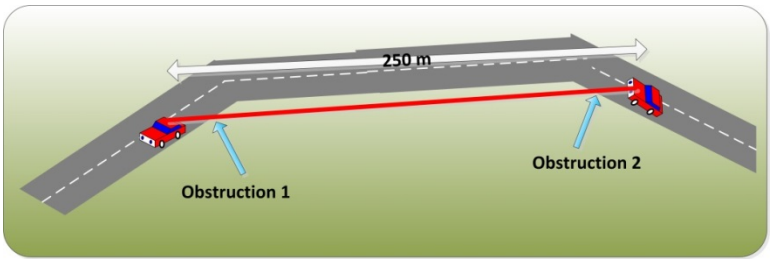

Fig. 5. Connection Loss in FSC6

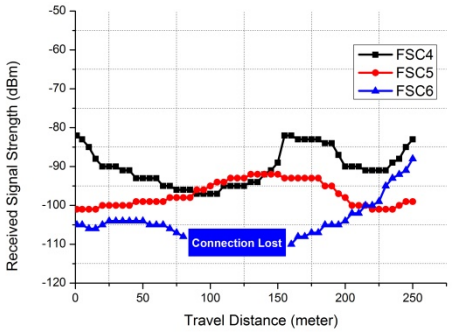

Fig. 6. RSS in FSC4, FSC5 and FSC6

In another arrangement, both the communicating vehicles were driven at variable speeds in such a manner that Tx was 150 meters ahead of Tr at the start of the test. The inter-vehicular distance began to shrink as Tr (with greater speed) started to approach Tx. Tr approximately covered 16 meters every second while Tx only covered 8 meters in each second. The communicating vehicles lose the LOS with each other in the beginning of the test. However, due to the greater speed of Tr, the two vehicles came in LOS with each other afterwards. Therefore, the RSS started to increase as Tr approached Tx. The RSS increased to a maximum level and then started to decline as the Tr passed Tx. The change in RSS in FSC7 is shown in **Fig. 7**.

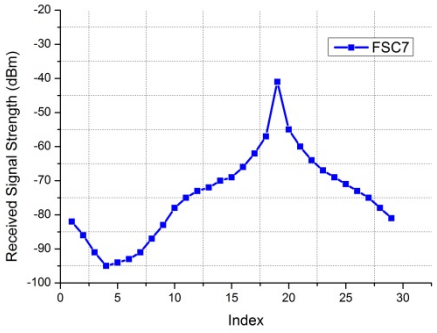

Fig. 7. RSS in FSC7

Fig. 8 shows the RSS in USC1 and USC2 where Tx was kept stationary at the start of the underpass and Tr was driven at a very low speeds (5 km/hr in USC1 and 20 km/hr in USC2) in order to carefully obtained the RSS values after each meter along the underpass. Furthermore, these tests were carried out to observe the impact of variable Tr speed inside the underpass and

on the straight road just after the underpass. As, the selected underpass was a part of busy and major urban road in a metropolitan city, therefore, the speed of Tr was kept in a range which is followed by the usual traffic on which use the selected underpass. A decrease in RSS up to approximately 40 dBm is observed with in the first 20 meters of the measurement inside the underpass. However, when the Tr moved a few meters outside the underpass, the fluctuation in RSS became stable and a gradual decrease in RSS was observed. The phenomenon of gradual decrease and relatively stable RSS values can be seen in **Fig. 8** when the distance between communicating vehicles exceed 30 meters in both USC1 and USC2. However, the different speeds of Tr in USC1 and USC2 seems to have no major effect on the RSS values.

In USC3, the communicating vehicles are driven with the same speed maintaining a distance of 15 meters between them. This test is carried out to observe the change in attenuation as the one or both of the vehicles enter in the underpass. Both the vehicles start their journey on the straight road 15 meters away from the underpass and then enter into the underpass one after another. As, the two vehicles are separated by a predefined distance, no dramatic change in the RSS is observed.

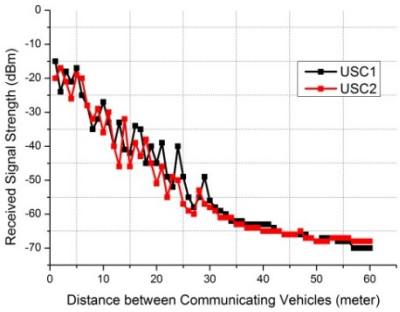

Fig. 8. RSS in USC1 and USC2

However, due to the waveguide-effect resulting from the structure of the underpass, diverse change in the RSS with the overall increase in the RSS is observed as the vehicles enter into the underpass one after the other. The fluctuation in the RSS values was soon balanced as the vehicles left the underpass. The same arrangement of USC3 is repeated in USC4 by maintaining a larger distance (25 meters) between the communicating vehicles. One of the vehicles was kept 25 meters away from the entrance of the underpass maintaining a further distance of 25 meters with the other vehicle. An increase in RSS is observed as the vehicles enter the underpass one after the other. This increase in RSS was at the highest level when both the vehicles were inside the underpass. However, a decrease in RSS was monitored when the two vehicles left the underpass. The change in RSS in USC3 and USC4 is shown in **Fig. 9**.

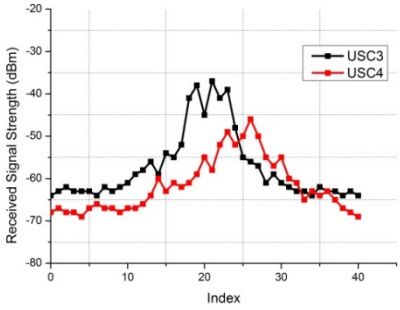

Fig. 9. RSS in USC3 and USC4

In USC5, both the communicating vehicles were driven at variable speeds (Tx with 15 km/hr and Tr with 30 km/hr) in such a manner that Tx was 30 meters ahead of Tr initially. The inter-vehicular distance began to reduce as Tr (with greater speed) started to approach Tx. Both the vehicles were inside the underpass after approximately 8 seconds from the start of the test. Therefore, a sharp increase in the RSS is observed as both the communicating vehicles were not only inside the underpass but were also very close to each other as Tr overtakes Tx. However, the RSS increased to a maximum level and then started to decline as the Tr passed Tx and continually went further away from Tx. In the process, both Tx and Tr left the underpass on to the straight road ahead. The change in RSS in USC5 is shown in **Fig. 10**.

Relatively high path loss is observed in NLOS conditions as compared to LOS conditions, therefore, maintaining LOS can improve vehicular communication. Hence, the utilization and placements of RSUs at optimal positions can reduce path loss.

5. Validation

The physical sites selected for field measurements are reproduced in simulation environment by importing the road topologies from the web-based OpenStreetMap utility into the traffic simulator SUMO [30]. The output of SUMO is further fed to the custom-built java discrete event simulator that scans the output from SUMO and applies the proposed propagation formulas for the respective flyover and underpass in order to produce the predicted path loss. The proposed RPM is validated by comparing the predicted path loss with the real-world data obtained from the field measurement campaign on flyover and underpass. The RSS values from the real-world testing in multiple scenarios is converted to the path loss and compared with the predicted path loss. To apply the proposed formulas for the flyover, we divided the path loss values in to two groups; LOS path loss and NLOS path loss.

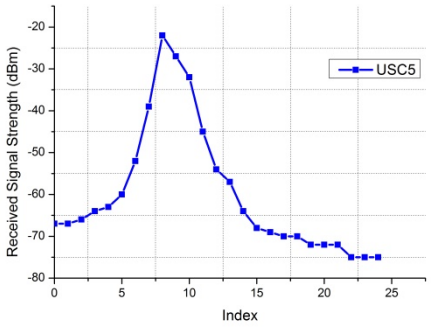

Fig. 10. RSS in USC5

In LOS path loss, two components participating in total path loss were considered namely, (a) free space path loss, (b) additional attenuation caused by the moving radio obstacles. There was low frequency of moving radio obstacles because the actual site of the measurement campaign was a part of busy urban roadway and the mass transportation system (Metro Bus) has its own elevated track. Therefore, the additional attenuation caused by moving radio obstacle had a little impact on the total LOS path loss on the particular selected site for field measurement. Hence, the value of F is considered to be 0.1 to compare the predicted value of path loss with the actual measurement results for LOS scenario.

A relatively high additional signal attenuation ($\beta = \sim 14$dB) was observed due to the heavy and wide concrete material used on the two outer edges of the flyover, Therefore, the edges of

the flyover acted as static radio obstacles with a higher impact on signal attenuation in NLOS path loss. The pillars of the flyover did not obstruct the LOS between the communicating vehicles because the measurements were performed on the extreme left lane. Therefore, the impact of pillars in NLOS scenario was neglected in this particular situation.

The predicted path loss values for the flyover are compared with the measured results in multiple scenarios to validate the proposed formulas designed specifically for the flyovers. The increase in the predicted path loss with the increase in inter-vehicular distance is monitored and compared with measurement values of the path loss on flyover. A comparison among predicted path loss values and measured results obtained from the field measurement campaign is shown in **Fig. 11** that depicts a close agreement between the measured and predicted values of path loss for flyover. The R^2 value as obtained by the statistical analysis yield **0.94** that confirms the applicability of the proposed RPM to predict path loss in flyover for vehicular communication. A residual analysis on the path loss data was also performed and no clear pattern was observed. Furthermore, a remarkable average accuracy of 97% was observed when the predicted path loss values were compared with the measured path loss values. The R^2 value, the residual analysis and the average accuracy reaffirmed the suitability of the proposed RPM to predict path loss on flyovers for the frequency band suitable for VANETs.

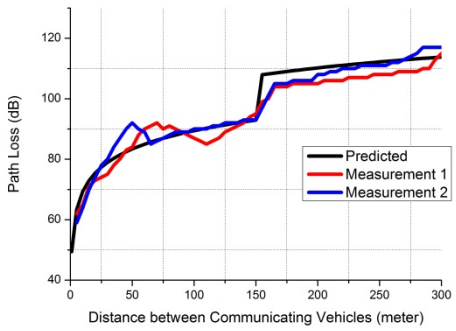

Fig. 11. Path Loss on Flyovers (Measured vs Predicted)

To apply the proposed formulas for the underpass, we divided the path loss values in to three groups; group A (when both the communicating vehicles driven inside the underpass), group B (when only one of the communicating vehicles is been inside and the other vehicle is outside the underpass) and group C (when both the communicating vehicles are outside on two different ends with the architecture of the underpass between them). In the group A, the major participating path loss factors were the dimension of the underpass and the distance between the communicating vehicles. The communication inside the underpass was merely disturbed by the moving radio obstacles because of the low frequency of the large moving vehicles in the selected underpass. Likewise, the communicating vehicles were in LOS with each other in group B as well, therefore, the major factors participating in the total path loss were; (a) free space path loss utilizing the effective distance $\boldsymbol{d_{eu}}$ between the communicating vehicles and (b) additional attenuation caused by the moving radio obstacles. Due to the low frequency of large moving vehicles, additional attenuation due to other vehicles was not on a large scale in group B as well. In group C, the whole length of the underpass is considered to obtain the effective distance $\boldsymbol{d_{eu}}$ between the communicating vehicles.

The predicted path loss values for the underpass are compared with the measured RSS values resulting from the underpass experiment to validate the proposed RPM for underpass.

The increase in the predicted path loss with the increase in inter-vehicular distance is monitored and compared with measurement values of the path loss in underpass. A comparison among predicted path loss values and measured results obtained from the field measurement campaign for underpass is shown in **Fig. 12** that depicts a close agreement between the measured and predicted values of path loss for underpass. The R^2 value yield **0.94** that affirms the suitability of the proposed RPM in the estimation of the path loss in underpasses for effective vehicular communication. A residual analysis on the path loss data was also performed and no clear pattern was observed. Furthermore, an average accuracy of **91%** was calculated when the predicted path loss values were compared with the measured path loss values. The R^2 value, the residual analysis and the average accuracy reaffirmed the suitability of the proposed RPM to predict path loss in underpass.

6. Comparison of Existing and Proposed RPMs

The existing RPMs employed in VANETs do not consider the structure of the flyover as a potential radio obstacle and the positive effects of an underpass on the signal propagation. Therefore, they lack in predicting path loss accurately for the communicating vehicles that are travelling on the flyover and inside the underpass. Three widely used existing RPMs (free space model, two ray ground model and CORNER) are selected and compared with the proposed RPM on the basis of path loss and PDR using simulation.

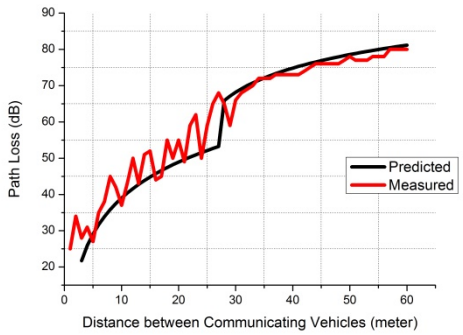

Fig. 12. Path Loss in Underpass (Measured vs Predicted)

6.1 Simulation Setup

To compare the proposed RPM with the existing RPMs, multiple simulators were used to accommodate for the real road environment within the simulation. Like the simulation used in validation to produce the predicted path loss, the same platform (SUMO along with custom-built java discrete event simulator) was used to compare the proposed RPM with the existing RPMs where the traffic simulator (SUMO) facilitated the modelling of intermodal traffic systems and the same physical sites selected for field measurements are reproduced in SUMO by using web-based OpenStreetMap utility. The custom-built java discrete event simulator was equipped with propagation formulas for the proposed RPM as well as the existing RPMs (free space, two ray ground, CORNER). Hence, serving as a network simulation platform to simulate radio propagation in physical layer and the results are produced based in terms of path loss and PDR. The simulation environment was configured with 50 pairs of vehicles (total: 100 vehicles), wherein a transmitter and a receiver constituted one pair. Moreover, the transmitters within each pair were configured to transmit messages at

10 Hz. Note that, for the sake of analysis, transmissions from transmitters are only recorded at their respective receivers. The simulation time for the flyover and the underpass scenario was set at 400 and 300 seconds respectively.

6.2 Comparison Results (Flyover)

A comparison among the path loss predicted by proposed and existing RPMs is shown in **Fig. 13**. The free space model only predicts the path loss when the communicating vehicles are in LOS with each other. However, due to relative height of the flyover at different locations, the communicating vehicles even travelling on a straight line have a tendency to lose LOS among them. The existing RPMs consider a two dimensional plane and do not contemplate height of the flyover in estimating path loss. CORNER uses free space model in estimating the path loss in LOS scenario and two-ray ground model underestimates the path loss for the shorter distances. Therefore, all three of the considered existing RPMs are unable to predict the accurate path loss for the vehicular communication on flyovers. On the other hand, the proposed RPM accounts for the additional attenuation caused by multiple NLOS conditions for the communicating vehicles travelling on the flyover. The communicating vehicles in NLOS scenarios on opposite sides of the flyover may lose effective communication due to repeated obstructions resulting from the edges and pillars of the flyover. This phenomenon is only modeled in proposed RPM as opposed to existing RPMs. Abrupt increase in path loss predicted by proposed RPM can be seen in Fig. 13. No existing RPM considers the abrupt change in path loss because of the NLOS condition between the communicating vehicles travelling on the flyover.

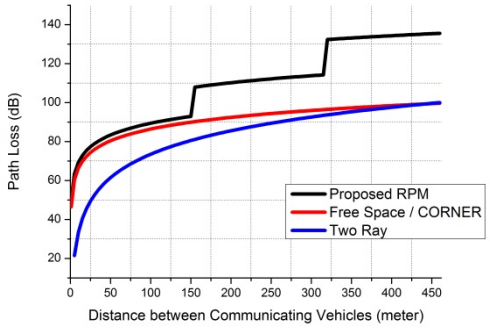

Fig. 13. Comparison of RPMs (Flyover)

A comparison among the PDR predicted by applying existing and proposed RPMs in flyover is also performed using the simulation. The comparison results for the flyover in terms of PDR are shown in **Fig. 14**. Unrealistic values of PDR in a high range (greater than 90%) are predicted for the flyover using the three existing RPMs because they only consider LOS scenario among the communicating vehicles and the signal attenuation caused by the structure of the flyover and the additional attenuation due to large moving vehicles is not contemplated by the exiting RPMs. On the other hand, the proposed RPM not only considers the structure of a flyover as a potential radio obstacle but also takes into account the additional signal attenuation due to the large moving obstacles. Therefore, the PDR values predicted by using the proposed RPM are in a relatively very low threshold (less than 40%). Hence, the analysis of proposed RPM advocates the inclusion of an RSU placed at the optimal position on the flyover in order to provide a reliable communication infrastructure for the vehicles communicating and driving along a flyover.

A one-way analysis of variance (ANOVA) is conducted to explore the path loss prediction efficiency of RPMs (proposed RPM, two-ray and CORNER) under flyover condition using SPSS version 18. ANOVA is used here to determine whether there are any significant differences between the path loss predicted by RPMs which in return highlight the RPM that accurately predict the path loss. A comparison of the mean predicted path loss of the considered RPMs is made using ANOVA to determine whether any of those means are significantly different from each other. A statistically significant difference between the models: $F(2, 273) = 70.74$, $p = .000$ was found between the predicted mean values of the considered RPMs. Here, the p-value showed that the differences between the means are statistically significant. Post-hoc comparisons using the Tukey HSD test indicated that the mean score for proposed RPM ($M = 109.97$, $SD = 20.25$) was significantly different from two-ray model ($M = 83.26$, $SD = 16.05$) and CORNER model ($M = 91.30$, $SD = 8.03$). CORNER behaves like free space model in LOS scenario, therefore, free space model is not considered in the statistical analysis. The highest mean value of predicted path loss is calculated by the proposed RPM showing that it considers the additional attenuation due to flyover structure and moving radio obstacles. Hence the proposed RPM realistically predicts the path loss on the flyover as compared to free space, two ray and CORNER.

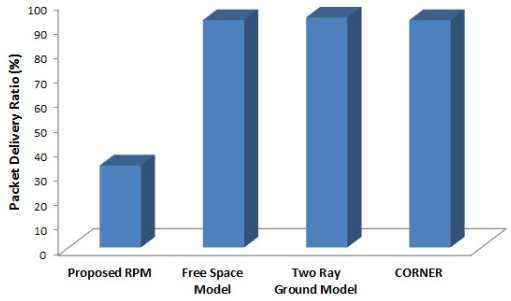

Fig 14. Comparison among Predicted PDR (Flyover)

6.3 Comparison Results (Underpass)

A comparison among the path loss predicted by existing and proposed RPMs is shown in **Fig. 15**. The free-space model over-estimates the path loss in underpass because the underpass geometry is not considered. Same is the case with CORNER as it utilizes free-space model to predict path loss in LOS scenario. However, two-ray model under-estimates the path loss when the vehicles are communicating inside the underpass but this path loss estimation becomes unrealistic when only one of the communicating vehicles is inside the underpass.

The proposed RPM specifically calculates the path loss for the communicating vehicles which are inside or near to an underpass and it also accounts for the additional signal attenuation caused by the large moving obstacles. Therefore, the proposed RPM predicts the path loss accurately for the situations where at least one of the vehicles is inside the underpass or both the vehicles are outside the underpass on opposite sides. The comparison results showed that the existing RPMs (free space, CORNER) either over-estimate the path loss or under-estimate (two-ray) it. Unlike, the existing RPMs, the proposed RPM keeps track of the positive effects of the underpass dimensions on the signal propagation and calculates effective distance to predict path loss. Therefore, the proposed RPM is more suitable to predict path loss for underpass environment as compared to existing RPMs in VANETs. A comparison among the PDR predicted by the applying existing and the proposed RPMs in underpass is also

performed. However, due to small length of the underpass (27 meters), the exiting as well as the proposed RPM predicts the maximum PDR. Therefore, its plot is not shown.

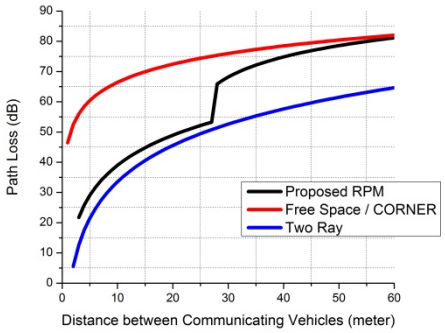

Fig. 15. Comparison of RPMs (Underpass)

ANOVA is conducted to explore the path loss prediction efficiency of considered RPMs in underpass scenario as well. Like the flyover scenario, a statistically significant difference between the models: $F(2, 171) = 51.06$, $p = .000$. Post-hoc comparisons using the Tukey HSD test indicated that the mean score for proposed RPM ($M = 61.38$, $SD = 17.75$) was significantly different from two ray model ($M = 49.81$, $SD = 12.90$) and CORNER ($M = 74.57$, $SD = 6.45$). The mean value of predicted path loss calculated by the proposed RPM is less than CORNER showing that the proposed RPM considers the positive effects of underpass structure on signal attenuation. Hence the proposed RPM realistically predicts the path loss in underpass as compared to existing RPMs.

7. Conclusion and Future Work

This paper presents RPM for vehicular communication on flyovers and inside the underpasses. The proposed RPM considers the impact of flyover's structure on the RSS. The proposed RPM also utilizes the simple geometric characteristics of the underpass along with the radio signal's wavelength to predict the major component of the path loss in underpass. The impact of large moving vehicles on the radio propagation is also considered in the proposed RPM and additional path loss component due to single knife-edge diffraction from the moving radio obstacles is added to predict the total path loss. Moreover, a field measurement campaign using 5 GHz frequency band was carried out in order to physically measure the RSS and the path loss. During the field measurement campaign, multiple arrangements of communicating nodes were utilized having different speeds and variable inter-vehicular distances. The predicted path loss from the proposed RPM is found to be in a close agreement with the measured results obtained from the field measurement campaign. The proposed RPM is also compared with exiting RPMs in terms of path loss prediction and PDR. This study utilized Wifi devices configured at 5 GHz for field measurement; the same tests are to be repeated using 802.11p transceivers at 5.9 Ghz frequency band in order to further affirm the suitability of the model for the vehicular communication.

References

[1] M. Boban, T. T. Vinhoza, M. Ferreira, J. Barros, and O. K. Tonguz, "Impact of vehicles as obstacles in vehicular ad hoc networks," *IEEE Journal on Selected Areas in Communications,* vol. 29, pp. 15-28, 2011. Article (CrossRef Link)

[2] S. A. A. Shah, M. Shiraz, M. K. Nasir, and R. B. M. Noor, "Unicast routing protocols for urban vehicular networks: review, taxonomy, and open research issues," *Journal of Zhejiang University SCIENCE C*, vol. 15, pp. 489-513, 2014. Article (CrossRef Link)

[3] J. B. Kenney, "Dedicated short-range communications (DSRC) standards in the United States," in *Proc. of the IEEE*, vol. 99, pp. 1162-1182, 2011. Article (CrossRef Link)

[4] M. A. Qureshi and R. Md Noor, "Towards improving vehicular communication in modern vehicular environment," in *Proc. of 11th Int. Conf. on Frontiers of Information Technology (FIT)*, pp. 177-182, 2013. Article (CrossRef Link)

[5] A. Hrovat, G. Kandus, and T. Javornik, "Four-slope channel model for path loss prediction in tunnels at 400 MHz," *Microwaves, Antennas & Propagation, IET*, vol. 4, pp. 571-582, 2010. Article (CrossRef Link)

[6] E. Giordano, R. Frank, G. Pau, and M. Gerla, "Corner: A radio propagation model for vanets in urban scenarios," in *Proc. of the IEEE*, vol. 99, pp. 1280-1294, 2011. Article (CrossRef Link)

[7] R. H. Khokhar, T. Zia, K. Z. Ghafoor, J. Lloret, and M. Shiraz, "Realistic and efficient radio propagation model for V2X communications," *KSII Transactions on Internet and Information Systems (TIIS)*, vol. 7, pp. 1933-1954, 2013. Article (CrossRef Link)

[8] M. A. Qureshi, R. M. Noor, S. Shamshirband, S. Parveen, M. Shiraz, and A. Gani, "A Survey on Obstacle Modeling Patterns in Radio Propagation Models for Vehicular Ad Hoc Networks," *Arabian Journal for Science and Engineering*, vol. 40, pp. 1385-1407, 2015. Article (CrossRef Link)

[9] Z. Changsen and M. Yan, "Effects of cross section of mine tunnel on the propagation characteristics of UHF radio wave," in *Proc. of 7th Intl. Symposium on Antennas, Propagation & EM Theory*, pp. 1-5, 2006. Article (CrossRef Link)

[10] Y. Yamaguchi, T. Abe, and T. Sekiguchi, "Radio wave propagation loss in the VHF to microwave region due to vehicles in tunnels," *IEEE Transactions on Electromagnetic Compatibility,* vol. 31, pp. 87-91, 1989. Article (CrossRef Link)

[11] Y. Zhang, "Natural propagation of radio signals in confined spaces," *Microwave and Optical Technology Letters*, vol. 23, pp. 38-42, 1999. Article (CrossRef Link)

[12] S. Kaul, K. Ramachandran, P. Shankar, S. Oh, M. Gruteser, I. Seskar, and T. Nadeem, "Effect of antenna placement and diversity on vehicular network communications," in *Proc. of 4th Annual IEEE Communications Society Conf. on Sensor, Mesh and Ad Hoc Communications and Networks*, pp. 112-121, 2007. Article (CrossRef Link)

[13] M. Rehmani, A. Rachedi, S. Lohier, T. Alves, and B. Pousso, "On the feasibility of making intelligent antenna selection decision in IEEE 802.15. 4 wireless sensor networks," in *Proc. of Computing, Communications and IT Applications Conference (ComComAp)*, pp. 41-46, 2013. Article (CrossRef Link)

[14] J. B. Andersen, T. S. Rappaport, and S. Yoshida, "Propagation measurements and models for wireless communications channels," *IEEE Communications Magazine*, vol. 33, pp. 42-49, 1995. Article (CrossRef Link)

[15] H. T. Friis, "A note on a simple transmission formula," in *Proc. of IRE*, vol. 34, pp. 254-256, 1946. Article (CrossRef Link)

[16] G. E. Athanasiadou, A. R. Nix, and J. P. McGeehan, "A microcellular ray-tracing propagation model and evaluation of its narrow-band and wide-band predictions," *IEEE Journal on Selected Areas in Communications,* vol. 18, pp. 322-335, 2000. Article (CrossRef Link)

[17] M. Catedra, J. Perez, F. de Adana, and O. Gutierrez, "Efficient ray-tracing techniques for three-dimensional analyses of propagation in mobile communications: application to picocell and microcell scenarios," *IEEE Antennas and Propagation Magazine,* vol. 40, pp. 15-28, 1998. Article (CrossRef Link)

[18] T. S. Rappaport, *Wireless communications: principles and practice* vol. 2: prentice hall PTR New Jersey, 1996.
[19] B. Sklar, "Rayleigh fading channels in mobile digital communication systems. I. Characterization," *IEEE Communications Magazine*, vol. 35, pp. 90-100, 1997. Article (CrossRef Link)
[20] F. J. Martinez, C.-K. Toh, J.-C. Cano, C. T. Calafate, and P. Manzoni, "Realistic radio propagation models (RPMs) for VANET simulations," in *Proc. of IEEE Wireless Communications and Networking Conference*, pp. 1-6. 2009. Article (CrossRef Link)
[21] A. Mahajan, N. Potnis, K. Gopalan, and A. Wang, "Modeling vanet deployment in urban settings," in *Proc. of the 10th ACM Symposium on Modeling, analysis, and simulation of wireless and mobile systems*, pp. 151-158, 2007. Article (CrossRef Link)
[22] C. Sommer, D. Eckhoff, R. German, and F. Dressler, "A computationally inexpensive empirical model of IEEE 802.11 p radio shadowing in urban environments," in *Proc of. 8th Intl. Conf. on Wireless On-Demand Network Systems and Services*, pp. 84-90, 2011.
[23] Q. Sun, S. Y. Tan, and K. C. Teh, "Analytical formulae for path loss prediction in urban street grid microcellular environments," *IEEE Transactions on Vehicular Technology*, vol. 54, pp. 1251-1258, 2005. Article (CrossRef Link)
[24] A. Hrovat, G. Kandus, and T. Javornik, "A survey of radio propagation modeling for tunnels," *IEEE Communications Surveys & Tutorials*, vol. 16, pp. 658-669, 2014. Article (CrossRef Link)
[25] Y. P. Zhang, "Novel model for propagation loss prediction in tunnels," *IEEE Transactions on Vehicular Technology,*, vol. 52, pp. 1308-1314, 2003. Article (CrossRef Link)
[26] L. Deryck, "Natural propagation of electromagnetic waves in tunnels," *IEEE Transactions on Vehicular Technology*, vol. 27, pp. 145-150, 1978. Article (CrossRef Link)
[27] R. Wang and J. Feng, "Grid-based Correlation Localization Method in Mixed Line-of-Sight/Non-Line-of-Sight Environments," *KSII Transactions on Internet and Information Systems (TIIS)*, vol. 9, pp. 87-107, 2015.
[28] M. A. Qureshi, R. M. Noor, A. Shamim, S. Shamshirband, and K.-K. R. Choo, "A Lightweight Radio Propagation Model for Vehicular Communication in Road Tunnels," *PloS one*, vol. 11, p. e0152727, 2016. Article (CrossRef Link)
[29] B. Chazelle and H. Edelsbrunner, "An optimal algorithm for intersecting line segments in the plane," *Journal of the ACM (JACM)*, vol. 39, pp. 1-54, 1992. Article (CrossRef Link)
[30] M. Behrisch, L. Bieker, J. Erdmann, and D. Krajzewicz, "SUMO–Simulation of Urban MObility," in *Proc. of. 3rd Intl. Conf. on Advances in System Simulation (SIMUL 2011), Barcelona, Spain*, 2011.

Muhammad Ahsan Qureshi received his MCS degree from the University of Arid Agriculture, Pakistan in 2001. He received his MS(CS) degree in 2009 from COMSATS Institute of Information Technology (CIIT), Islamabad and joined as a Lecturer in Federal Urdu University of Arts, Science and Technology, Islamabad. He completed his PhD from Department of Computer System and Technology, Faculty of Computer Science & Information Technology, University of Malaya, Kuala Lumpur, Malaysia in 2016. His research interests include Wireless and Mobile communication, VANETs, Algorithms and Computing.

Ehsan Mostajeran is student at the Faculty of Computer Science and Information Technology (FSKTM), University of Malaya, Kuala Lumpur, Malaysia. His research interests include Distributed Computing, Computer Communication, Networks and Electronic Engineering.

Rafidah Md Noor is an Associate Professor at the Faculty of Computer Science and Information Technology, University of Malaya, Kuala Lumpur, Malaysia. She received her BIT from University Utara Malaysia in 1998, and MSc in Computer Science from University Technology Malaysia in 2000, and PhD in Computing from Lancaster University, United Kingdom in 2010. Rafidah's research is related to field of transportation system in computer science research domain, including vehicular networks, traffic management systems, wireless sensor networks, Quality of Service and Quality of Experience. Rafidah has performed nearly RM665,606.00 for High-Impact Research, Ministry of Education (HIR-MOE) grant and other research grants from the University of Malaya and public sectors such as FRGS and E-Science. She has several collaborators from China, Taiwan, South Korea, France, Australia, and United Kingdom who are willing to support in providing excellent research outputs. She has supervised more than 20 postgraduate students within 5 years. She has published 20 journals in Science Citation Index Expanded, 10 journals in Non-Science Citation Index, 45 proceeding articles published in International conferences and a few book chapters.

Azra Shamim is an Assistant Professor at the COMSATS Institute of Information Technology, Islamabad, Pakistan. She received her PhD degree from Faculty of Computer Science and Information Technology (FSKTM), University of Malaya, Kuala Lumpur, Malaysia in 2015, and MSCS from the COMSATS Institute of Information Technology, Islamabad, Pakistan in 2009, and BSCS (Hons) from the university of Arid Agriculture, Rawalpindi, Pakistan in 2006. Her research interests are Wireless Networks, Data Mining and Information Processing.

Chih-Heng Ke received his B.S. and Ph.D degrees in electrical engineering from National Cheng-Kung University, in 1999 and 2007. He is an associate professor at the Department of Computer Science and Information Engineering in National Quemoy University, Kinmen, Taiwan. His current research interests include Multimedia Communications, Wireless Networks, and Software defined Networks.